A fast preamplifier concept for SiPM-based time-of-flight PET detectors

Huizenga, J; Seifert, S; Schreuder, F; van Dam, HT; Dendooven, P; Lohner, H.; Vinke, R; Schaart, DR

DOI
10.1016/j.nima.2011.11.012

Publication date
2012

Document Version
Accepted author manuscript

Published in
Nuclear Instruments & Methods in Physics Research. Section A: Accelerators, Spectrometers, Detectors, and Associated Equipment

Citation (APA)
Huizenga, J., Seifert, S., Schreuder, F., van Dam, HT., Dendooven, P., Lohner, H., Vinke, R., & Schaart, DR. (2012). A fast preamplifier concept for SiPM-based time-of-flight PET detectors. *Nuclear Instruments & Methods in Physics Research. Section A: Accelerators, Spectrometers, Detectors, and Associated Equipment*, *695*, 379-384. https://doi.org/10.1016/j.nima.2011.11.012

Nuclear Instruments and Methods in Physics Research A ▮ (▮▮▮▮) ▮▮▮–▮▮▮

Contents lists available at SciVerse ScienceDirect

Nuclear Instruments and Methods in Physics Research A

journal homepage: www.elsevier.com/locate/nima

A fast preamplifier concept for SiPM-based time-of-flight PET detectors

J. Huizenga [a,*], S. Seifert [a], F. Schreuder [b], H.T. van Dam [a], P. Dendooven [b], H. Löhner [b], R. Vinke [b], D.R. Schaart [a]

[a] Delft University of Technology, Radiation Detection & Medical Imaging, Mekelweg 15, 2629 JB Delft, The Netherlands
[b] Kernfysisch Versneller Instituut, University of Groningen, Zernikelaan 25, 9747 AA Groningen, The Netherlands

ARTICLE INFO

Keywords:
Silicon photomultiplier
Time-of-flight PET
Fast transimpedance amplifier

ABSTRACT

Silicon photomultipliers (SiPMs) offer high gain and fast response to light, making them interesting for fast timing applications such as time-of-flight (TOF) PET. To fully exploit the potential of these photosensors, dedicated preamplifiers that do not deteriorate the rise time and *signal-to-noise* ratio are crucial. Challenges include the high sensor capacitance, typically >300 pF for a 3 mm $\times$ 3 mm SiPM sensor, as well as oscillation issues. Here we present a preamplifier concept based on low noise, high speed transistors, designed for optimum timing performance. The input stage consists of a transimpedance common-base amplifier with a very low input impedance even at high frequencies, which assures a good linearity and avoids that the high detector capacitance affects the amplifier bandwidth. The amplifier has a fast timing output as well as a 'slow' energy output optimized for determining the total charge content of the pulse. The rise time of the amplifier is about 300 ps. The measured coincidence resolving time (CRT) for 511 keV photon pairs using the amplifiers in combination with 3 mm $\times$ 3 mm SiPMs (Hamamatsu MPPC-S10362-33-050C) coupled to 3 mm $\times$ 3 mm $\times$ 5 mm $LaBr_3$:Ce and LYSO:Ce crystals equals 95 ps FWHM and 138 ps FWHM, respectively.

1. Introduction

Silicon photomultipliers (SiPMs) consist of a large number of single-photon avalanche diodes (SPADs) or Geiger-mode avalanche photodiodes (GM-APDs), here referred to as microcells, all connected in parallel. SiPMs offer a high gain and a fast response to light, which makes them interesting for fast timing applications such as scintillation detectors for time-of-flight positron emission tomography (TOF-PET).

However, using SiPMs to their full potential is not trivial. For example, conventional amplifier techniques suitable for the readout of photomultiplier tubes (PMTs), photodiodes, or avalanche photodiodes (APDs), are not one-to-one applicable to SiPMs due to the very different electronic characteristics of these types of light sensor as described in the next section.

To achieve the best possible timing performance with SiPMs, dedicated preamplifiers are needed that do not deteriorate the rise time and *signal-to-noise* ratio of the SiPM signal. Here we present a SiPM preamplifier design concept based on low noise, high speed, discrete transistors.

2. Amplifier design considerations

2.1. SiPM electronic properties

Electronic modeling of SiPMs has been pioneered by Corsi et al. [1]. Seifert et al. [2] recently proposed an extended model and investigated two sensors from Hamamatsu in detail, viz. the 3 mm $\times$ 3 mm MPPC S10362-33-25C and the 1 mm $\times$ 1 mm MPPC S10362-11-25U. A main characteristic of these devices is their high terminal capacitance (>300 pF for the 3 mm $\times$ 3 mm device) consisting of the sum of all cell capacitances and the internal interconnect capacitance. Since this is much larger than the 3 pF–10 pF anode capacitance of a typical PMT [3], suboptimal performance may result if PMT preamplifiers are attached to SiPMs. Especially when high timing resolution is important the high capacitance of SiPMs needs to be accounted for.

Another characteristic of SiPMs is the dependence of the output impedance on the number of microcells being fired, in contrast with the almost ideal current source behavior of PMTs [3]. When several photons hit a SiPM at the same time, part of the microcells may discharge, while other cells remain inactive. Each cell has its own quench resistor, diode resistance, and adherent parasitic capacitances. The total impedance of a cell is very different depending on its state (inactive or discharging). Since all cells are connected in parallel, it follows that the SiPM output impedance varies with the amount of light incident on the sensor [2].

* Corresponding author.
E-mail address: j.huizenga@tudelft.nl (J. Huizenga).

0168-9002/$ - see front matter © 2011 Elsevier B.V. All rights reserved.
doi:10.1016/j.nima.2011.11.012

If a SiPM is connected to an amplifier with finite input impedance, its varying output impedance may give rise to non-linear behavior. Studies have shown that the linearity of the overall response improved with decreasing input impedance of the amplifier [2]. Together with the already mentioned effect of the high SiPM capacitance on the time response, one can conclude that the lower the preamplifier input impedance, the faster the temporal response and the better the linearity of the signal will be.

2.2. Voltage amplifier with shunt resistor

A common approach to amplify SiPM signals is to use a voltage amplifier in combination with a current-converting shunt resistor R, as shown in Fig. 1. However, if R is kept to a value of, for example, 10 Ω or smaller because of the reasons given in Section 2.1, the generated signal voltage across R will be very small, necessitating a high-gain amplifier. The small signal voltage furthermore requires this amplifier to exhibit very low noise in order not to degrade the *signal-to-noise* ratio.

Due to gain-bandwidth limitations, high-speed amplifiers typically have a relatively low gain of about 20 dB or less, requiring several of these amplifiers to be placed in cascade as in Fig. 2 to obtain a decently measurable signal. The effect of connecting multiple amplifiers in cascade, even if they all have the same bandwidth, is an increased curvature of the initial part of the pulse response [4]. In other words, the signal slope at the onset of the amplified pulse is decreased, which may result in significant worsening of the timing resolution, especially since the best timing with SiPM-based scintillation detectors is typically achieved using very low threshold values for time pick-off [5–7].

To illustrate this, the normalized simulated time responses of 4 cascaded amplifiers, all having an arbitrarily chosen bandwidth of 1 GHz, are shown in Fig. 3. Trace 0 is the initial input step voltage, while traces 1 to 4 are the output signals of amplifiers 1 to 4, respectively. The signal slope at 5% of the maximum amplitude is about 10 times lower for the 4th amplifier output than for the 1st amplifier output. The simulated bandwidth,

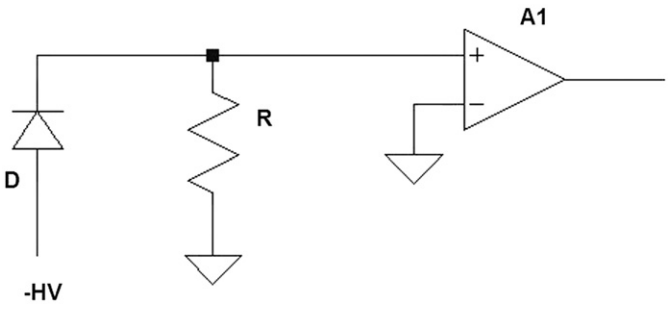

Fig. 1. Common SiPM readout scheme. A shunt resistor (R) converts the signal current from the reverse-biased (-HV) sensor (D) to a voltage, which is subsequently amplified by voltage amplifier A_1.

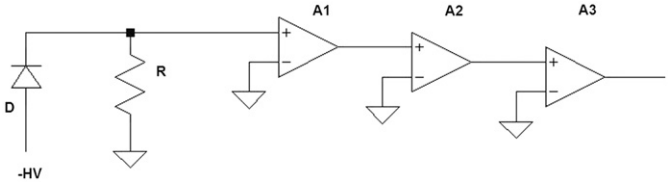

Fig. 2. Several cascaded amplifiers (A_1, A_2, A_3) increase the overall gain at the expense of increased curvature in the initial part of the pulse response.

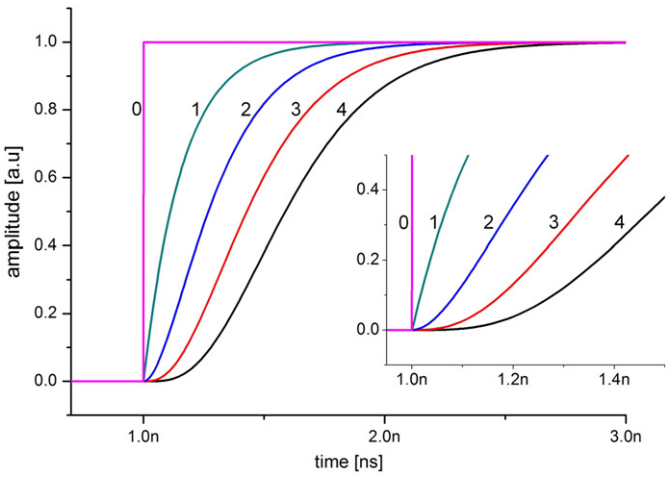

Fig. 3. Simulated transient response of 4 cascaded amplifiers, each having a bandwidth of 1 GHz. Traces 1 to 4 show the responses of amplifiers 1 to 4, respectively, to the initial step function at the input, represented by trace 0. The inset clearly shows a decreasing initial slope when the number of amplifiers is increased.

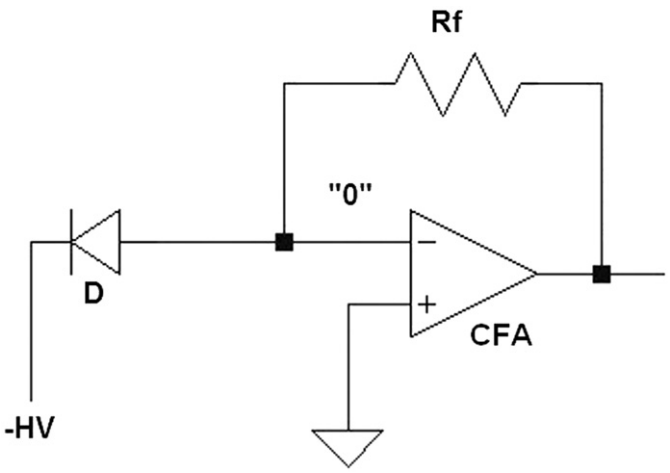

Fig. 4. Transimpedance amplifier based on a current-feedback operational amplifier (CFA). Resistor R_f converts the input signal current to an output voltage and typically is in the order of a few hundreds of ohm. The input impedance of the circuit can be close to zero ("0").

however, is only about 3 times lower, which means that for amplifier systems with multiple stages in cascade, considering bandwidth only can give a false impression of speed. Thus, the transient response should also be examined.

2.3. Transimpedance amplifier

In principle, a transimpedance amplifier might be expected to provide a suitable solution for both the high capacitance of the detector and the required low input impedance. Nowadays there are numerous high speed operational amplifiers with high bandwidth (>1 GHz), using which a transimpedance amplifier can easily be made. An example of such a circuit is shown in Fig. 4. Since the current-converting resistor R_f can be in the order of 100 Ω–500 Ω, the transimpedance gain of this amplifier can be high compared to the shunt resistor method. Most suitable [8] for high speed applications is the so-called current-feedback operational amplifier (CFA), which provides a true current input at the inverting terminal. The input impedance R_{int} of the inverting input is inherently low, in the order of 8 Ω–30 Ω for commercially available devices.

Please cite this article as: J. Huizenga, et al., Nuclear Instruments & Methods In Physics Research Section A (2011), doi:10.1016/j.nima.2011.11.012

Using feedback, the effective input impedance R_{eff} of the entire circuit is reduced to much lower values following the equation:

$$R_{eff} = \frac{R_{int}}{Z_0\beta + 1}$$

where Z_0 is the open-loop transimpedance gain and β the ratio of R_{int} and feedback resistor R_f. Z_0 can be 10^6 at low frequencies. Since the optimum value for the feedback resistor is in the order of 500 kΩ–1 kΩ for a CFA, β typically has a value of about 0.01 to 0.02, giving a $Z_0\beta$ in the order of 10^4, thus resulting in a very low value of R_{eff}.

Initial tests using an AD8000 CFA from Analog Devices and a R_f of 470 Ω have shown that the rise times obtained with such a circuit in combination with 3 mm × 3 mm SiPMs illuminated with a picosecond laser are longer than with a voltage amplifier with a small 5 Ω shunt resistor. The pulse shape also showed ringing, which can be explained by the reduced open-loop gain Z_0 at high frequencies. For example the AD8000 CFA has a Z_0 of ~200 at 1 GHz, giving a $Z_0\beta$ of only about 2–3. The result is a non-zero impedance at the virtual ground input (indicated as "0" in Fig. 4) for these frequencies.

Since the high sensor capacitance is also connected to the virtual ground the result is an increased rise time. Furthermore, the sensor capacitance together with the input resistance forms a reactive impedance, resulting in peaking of the gain at high frequencies and corresponding ringing of the output signal. For smaller sensors with a smaller capacitance (e.g. the MPPC S10362-11-25U), this amplifier has been shown to give good results [9].

2.4. Common-base amplifier

A common-base (also called grounded-base) amplifier without feedback is a good candidate to overcome the problems described in the preceding sections. Fig. 5 shows the basic scheme of a common-base amplifier. The emitter of the transistor forms the input of the amplifier. The base of the transistor has a DC biasing voltage but is decoupled to ground by means of a capacitor, in order to decrease the input impedance for signal frequencies.

By design, the input impedance is very small without using any feedback. The absence of feedback insures low input impedance even at very high frequencies, resulting in a negligible effect of the detector capacitance on the overall time response and minimizing non-linearity at the same time. The input signal current i flows from the emitter to the collector of the npn transistor and generates a voltage difference over the collector resistor R. Since the collector capacitance is very small, this resistor can be relatively large, enabling high transimpedance gain without compromising speed.

As compared to the shunt resistor method described in Section 2.2, the common base amplifier converts the signal current to a signal voltage that is at least an order of magnitude higher ($R = 100\ \Omega$). Furthermore, in the case of the shunt resistor method, the required fast time response dictates the choice of the shunt resistor since the response is a function of the detector capacitance and the shunt resistor value. In the case of the common base amplifier the resistor value can be chosen more freely since the detector capacitance is isolated from this resistor, as described in more detail in Section 3.1. The high gain results in less stringent noise demands on consecutive amplifiers and eliminates the need for multiple consecutive amplifying stages, thereby avoiding the increased curvature of the output pulse described in Section 2.2.

In the 1960s the common-base amplifier concept has already been introduced in nuclear electronics, although at that time with feedback [10]. The concept has also been used to read out resistive strip detectors [11] and high-speed photodiode optical interconnect applications [12–14]. A detailed description on the noise properties of a common base amplifier has been published by Hrisoho [15]. Recently, a comparable approach to read out SiPM sensors has been adapted by Corsi et al. [16], based on the CMOS technology.

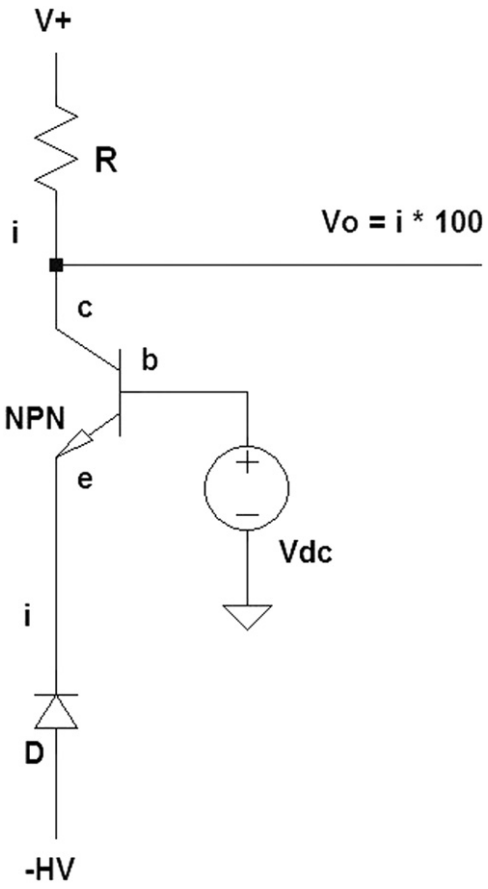

Fig. 5. Basic circuit of a common-base amplifier. The signal current i from the reverse-biased sensor D flows from the collector to the emitter and is transformed into a voltage by resistor R. The intrinsically low input impedance of the emitter isolates the detector capacitance from the remainder of the circuit, so that it does not affect the amplifier transfer function.

3. Materials and methods

3.1. Amplifier design

A common-base transimpedance amplifier for use with a 3 mm × 3 mm SiPM (Hamamatsu MPPC-S10362-33-050C) was built using discrete components selected for high speed (transition frequency in the order of 25 GHz) and low noise operation. To facilitate the measurements described in Section 3.2, it has a fast, sub-nanosecond timing output optimized for high time resolution as well as a 'slow' energy output with a bandwidth of ~10 MHz optimized for obtaining the total charge content of the pulse. The board design required high-frequency layout considerations in order to minimize series inductances and parasitic capacitances and to avoid oscillation problems.

The simplified circuit drawing of the amplifier is given in Fig. 6. The signals generated by the detector D are split into two parallel amplification branches using the filter network made up by R_s and C_s (33 Ω and 470 pF, respectively, in our design). The fast AC-coupled component of the signal is passed on to the

Please cite this article as: J. Huizenga, et al., Nuclear Instruments & Methods In Physics Research Section A (2011), doi:10.1016/j.nima.2011.11.012

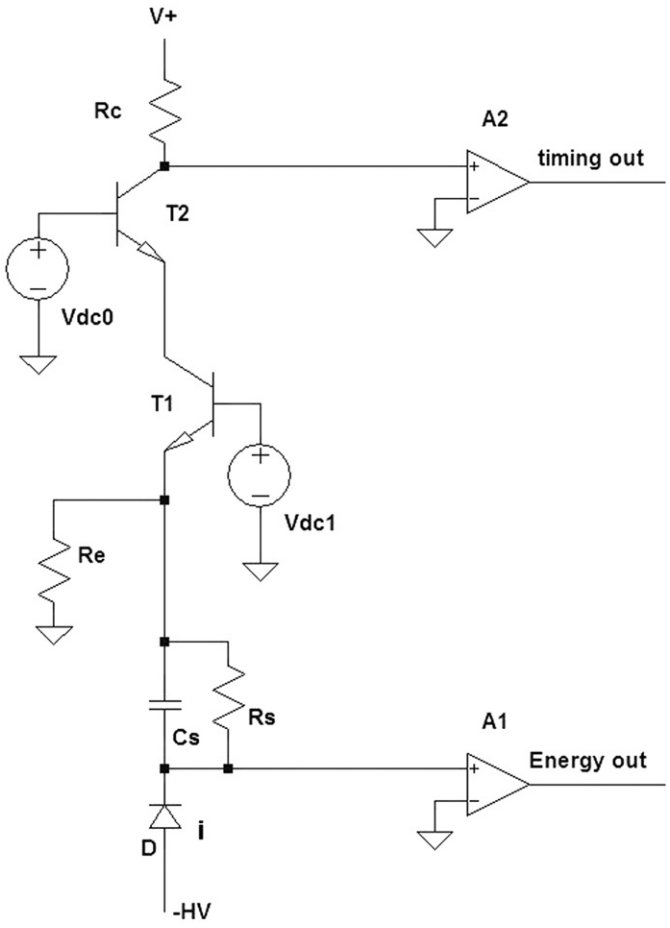

Fig. 6. Simplified circuit of the common-base SiPM amplifier built and tested in this work.

consecutive common-base amplifiers T_1 and T_2 and is further amplified and buffered by voltage amplifier A_2, forming the fast timing output.

In the second amplification branch a pre-shaped, slower signal is fed into amplifier A_1, providing the energy output. The shaped energy signal is optimized to meet the input specifications of commercially available pulse-shaping amplifiers to facilitate additional filtering and amplification. Both amplifier A_1 and A_2 are built using discrete components and are common-emitter amplifiers. The output impedance of both amplifiers is 50 Ω.

The bias current of transistors T_1 and T_2 is set using the resistor R_e (300 Ω in our design) and the base voltage V_{dc1}. The bias voltage at the emitter of T_1 is also present on the cathode of the reverse-biased detector D, enabling fine-tuning of the total detector bias voltage by changing the base voltage V_{dc1}, without changing the main bias voltage-HV. The fine-tuning option facilitates the use of a single main bias supply-HV if the elements of a SiPM array are read out in parallel using multiple amplifiers. The collector voltage of transistor T_1 can be adjusted independently for optimum performance using base voltage V_{dc0} of transistor T_2.

The current pulses i from the SiPM detector (diode D) flows from the collector of transistor T_1 to the emitter of transistor T_2. The circuit input impedance, which is inversely proportional to the DC collector current of transistor T_1, is about 5 Ω for a collector current of 5 mA and up to very high frequencies.

The current-to-voltage conversion takes place at the collector of transistor T_2, where the total capacitance is low, approximately 3 pF in our design. This capacitance together with the applied collector resistor R_c (100 Ω) determines the main time constant of the circuit. The influence of the high detector capacitance (>300 pF for the tested 3 mm × 3 mm SiPMs) on the circuit response is essentially eliminated.

3.2. Measurements

The amplifier intrinsic rise time was measured using current pulses, generated by coupling voltage pulses with a rise time of ~100 ps into the amplifier input via a capacitor. A dedicated circuit was made to enable connecting a 330 pF capacitance to the amplifier input in order to investigate the influence of the detector capacitance. The input impedance of this network was 50 Ω to match the output impedance of the pulse generator, while the output impedance was 1 Ω. The 330 pF capacitance was connected in series between this output, which virtually equals ground, and the input of the amplifier. An oscilloscope with a bandwidth of 3 GHz was used for this measurement. Spice simulations of the entire setup were performed and compared to the measurements.

The response to light pulses of the amplifier connected to a 3 mm × 3 mm SiPM was also tested. The pulses of a pico-second laser (Hamamatsu PLP-04, pulse width ~50 ps) were fed through optical filters such that ~30 cells of the SiPM were fired per pulse. The timing output of the amplifier was digitized using an Acqiris DC282 digitizer sampling at 8 Gs/s with a resolution of 10 bits.

The performance of the preamplifier in combination with SiPM-based scintillation detectors has also been tested. Full details of this experiment are described elsewhere [7]. In summary, a coincidence setup as shown in Fig. 7 was built using identical amplifiers connected to two SiPM detectors (Hamamatsu S10362-33-050c) placed at opposite sides of a Na-22 source of annihilation photon pairs. Tests were performed using $LaBr_3$:5%Ce crystals (Saint Gobain Brillance 380) or LYSO:Ce crystals (Crystal Photonics) with dimensions of 3 mm × 3 mm × 5 mm optically coupled to the SiPMs.

The fast timing signals were recorded using Acqiris DC282 digitizers sampling at 8 Gs/s with a resolution of 10 bits, while the energy signals were shaped and amplified using multichannel CAEN N568B amplifiers and digitized using a multichannel peak-sensing ADC (CAEN V785). Digital pulse traces for timing analysis were selected using the information of the peak-sensing ADCs. Only events in the full-energy peak, having energies between

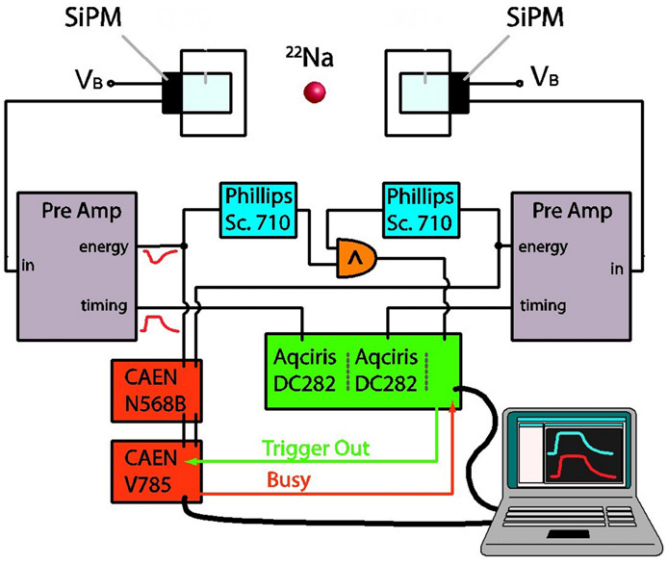

Fig. 7. Schematic representation of the coincidence setup.

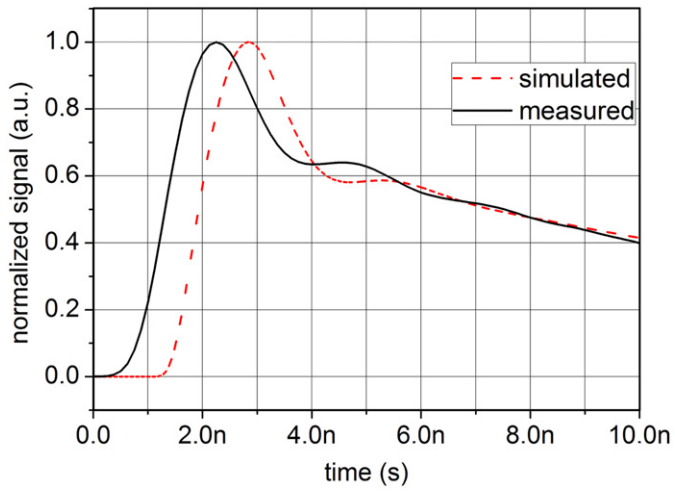

Fig. 8. Measured and simulated response to pulsed laser light of the combination of amplifier and SiPM (Hamamatsu MPPC-S10362-33-050C). The SiPM was illuminated with ~50 ps laser pulses, firing ~30 microcells per pulse. Both curves are normalized and the simulated trace is artificially delayed for better comparison.

490 keV and 532 keV, were accepted. Traces were analyzed offline to determine accurate time stamps as described in Ref. [7].

4. Results

Spice simulations of the circuit predicted output rise times in the order of ~300 ps in response to a pulsed current source connected to the input of the amplifier. The measured rise times indeed are equal to ~300 ps if a collector resistor R_c of 50 Ω is used (see Fig. 6) and with a 330 pF capacitance to ground at the amplifier input. When R_c is increased to 100 Ω the measured rise time increases to 550 ps, which is attributed to the remaining parasitic capacitance at the collector of transistor T_2. The simulated amplifier input impedance is 5 Ω up to a gigahertz, increasing to 7 Ω at 1.5 GHz and 50 Ω at 4 GHz.

The black, solid curve in Fig. 8 shows the digitized fast timing signal of the amplifier connected to a 3 mm × 3 mm SiPM in response to laser pulses. The red, dashed curve in the same figure indicates the response predicted by Spice simulations in which the amplifier is simulated together with a realistic Spice model of the SiPM detector [2] including parasitic inductances. The measured rise time is equal to about 1.05 ns, in good agreement with the value of 0.9 ns predicted by the Spice simulations.

The measured coincidence resolving time (CRT) for 511 keV annihilation photon pairs using the amplifiers in combination with 3 mm × 3 mm SiPMs coupled to 3 mm × 3 mm × 5 mm $LaBr_3$:Ce and LYSO:Ce crystals has been reported elsewhere [7] and equals 95 ps FWHM and 138 ps FWHM, respectively. These values were obtained using a low threshold value for time pick-off, showing the necessity of a fast initial curve. The threshold values are equal to about ~8 and ~3 equivalent single cell signal amplitudes for $LaBr_3$:Ce and LYSO:Ce, respectively.

5. Discussion and conclusion

We have developed a low-noise amplifier circuit that preserves the fast rise time of the signals produced by SiPM detectors. The low input impedance of this common-base amplifier ensures a minimum influence of the detector capacitance on the frequency response. Furthermore, due to the relatively high gain of the first amplification stage there is little need for additional amplification stages that might degrade the transient response. The design can easily be adapted to application-specific requirements on, for example, the desired gain, number of channels, and power dissipation.

Most of the power dissipation is due to the input transistor bias current required to obtain a low input impedance. If necessary the dissipation could be reduced using a feedback topology that lowers the input impedance [12–14]. A lower collector current could then be sufficient to obtain sufficiently low input impedance. However, in such a design one should avoid instabilities similar to those observed in current-feedback amplifiers.

The dominant pole of the circuit is created at the point where the signal current is transformed into a voltage, i.e. at the collector of the last transistor (T_2 in Fig. 6). The rise time of the output pulse in response to current pulses was found to increase from 300 ps to 550 ps when the collector resistor R_c was increased from 50 Ω to 100 Ω, indicating that the capacitance at the collector still forms a limiting factor and that some room remains for further improvement of the amplifier design.

One option for improvement would be to reduce the collector resistance, but this reduces the gain and would necessitate additional amplification stages, which is not recommendable. Another option would be to reduce the capacitance at the conversion point via layout modifications and/or by modifying amplifier A_2 in Fig. 6. At present this is a common-emitter amplifier whose collector-base capacitance is multiplied due to the Miller effect. A common-collector buffer followed by a common-emitter amplifier or a cascode amplifier might be a better solution since it does not suffer form the Miller effect, thus having a lower input capacitance.

Even though further improvements may still be possible, the present amplifiers enable excellent timing performance when applied in SiPM-based scintillation detectors. In previous studies, using a combination of a shunt resistor and a voltage amplifier to read out two 3 mm × 3 mm × 5 mm $LaBr_3$:Ce crystals coupled to 3 mm × 3 mm SiPMs [6], a CRT of ~100 ps FWHM was obtained. Repeating the same experiment with the shunt resistor and voltage amplifier replaced by the common-base amplifier yielded a CRT of ~95 ps FWHM [7], a small but significant improvement.

Moreover, the CRT obtained with equally sized LYSO:Ce crystals in the same setup improved from ~172 ps FWHM [5] to ~138 ps FWHM [7] when the new preamplifier was used. Although it cannot be fully excluded that other experimental factors also contribute to the observed differences, it is shown in Ref. [7] that the optimum threshold for time pick-off is significantly lower for LYSO:Ce than for $LaBr_3$:Ce. The low threshold makes the CRT more sensitive to both electronic noise and the signal slope at the onset of the output pulse. Hence, the advantages of the common-base amplifier concept are even more important for LYSO:Ce than for $LaBr_3$:Ce, which may explain the larger relative improvement of the CRT observed for LYSO:Ce.

Acknowledgments

This work was supported in part by Agentschap NL under Grant no. IS055019.

References

[1] F. Corsi, A. Dragone, C. Marzocca, A. Del Guerra, P. Delizia, N. Dinu, C. Piemonte, M. Boscardin, G.F. Dalla Betta, Nuclear Instruments and Methods in Physics Research, Section A 572 (2007) 416.
[2] S. Seifert, H.T. van Dam, J. Huizenga, R. Vinke, P. Dendooven, H. Löhner, D.R. Schaart, IEEE Transactions on Nuclear Science NS-56 (2009) 3726.
[3] A.G. Wright, The Use of Amplifiers with Photomultipliers, Electron Tubes Limited, Technical Reprint R/P094.

[4] H. Spieler, Semiconductor Detector Systems, 36, Oxford University Press, New York, 2005.
[5] S. Seifert, R. Vinke, H.T. van Dam, H. Löhner, P. Dendooven, F.J. Beekman, D.R. Schaart, IEEE Nuclear Science Symposium and Conference Record (2009) 2329.
[6] D.R. Schaart, S. Seifert, R. Vinke, H.T. van Dam, P. Dendooven, H. Löhner, F.J. Beekman, Physics in Medicine and Biology 55 (2010) 179.
[7] S. Seifert, H.T. van Dam, R. Vinke, P. Dendooven, H. Löhner, F.J. Beekman, D.R. Schaart, A comprehensive model to predict the timing resolution of SiPM-based scintillation detectors: theory and experimental validation, IEEE Transactions on Nuclear Science, in press.
[8] MT-060 Tutorial, 〈www.analog.com/static/imported-files/tutorials/MT-060.pdf〉, Analog Devices, 2009.
[9] S. Seifert, D.R. Schaart, H.T. van Dam, J. Huizenga, R. Vinke, P. Dendooven, H. Löhner, F.J. Beekman, IEEE Nuclear Science Symposium and Conference Record (2008) 1616.
[10] L.J. Herbst, Electronics for Nuclear Pulse Analysis, OUP, 1970. See article by A.B. Gillespie—Nuclear Pulse Amplifiers.
[11] E. Botta, D. Calvo, P. Cerello, C. Fanara, S. Marcello, O. Morra, Nuclear Instruments and Methods in Physics Research, Section A 383 (1996) 566.
[12] B. Wilson, I. Darwazeh, Electronics Letters 23 (1987) 88.
[13] T. Vanisri, C. Toumazou, IEEE Journal of Solid-State Circuits 30 (1995) 677.
[14] S.M. Park, S. Hong, IEEE Photonics Technology Letters 15 (8) (2003) 1138.
[15] A. Hrisoho, Time domain noise calculation for the common base current amplifier configuration, Nuclear Instruments and Methods 185 (1–3) 207–213, doi:10.1016/0029-554X(81)91213-1.
[16] F. Corsi, C. Marzocca, M. Foresta, G. Matarrese, A. Del Guerra, S. Marcatili, G. Llosa, G. Collazuol, G.F. Dalla Betta, C. Piemonte, Preliminary results from a current mode CMOS front-end circuit for silicon photomultiplier detectors, In: Proceedings of the 2007 IEEE Nuclear Science Symposium Conference Record N15-49, p. 360.

Please cite this article as: J. Huizenga, et al., Nuclear Instruments & Methods In Physics Research Section A (2011), doi:10.1016/j.nima.2011.11.012